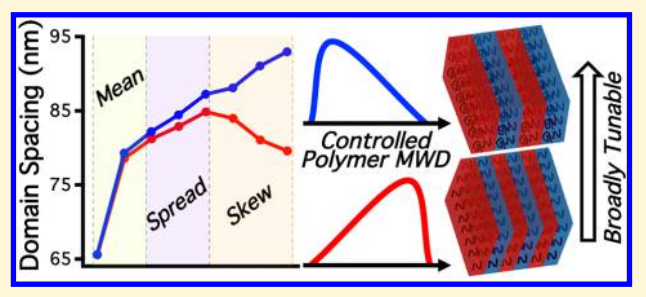
Exploiting Molecular Weight Distribution Shape to Tune Domain Spacing in Block Copolymer Thin Films

Dillon T. Gentekos, †,‡ Junteng Jia, †,‡ Erika S. Tirado, † Katherine P. Barteau, [§] Detlef-M. Smilgies, [⊥] Robert A. DiStasio, Jr.,*,† and Brett P. Fors*,†

Supporting Information

ABSTRACT: We report a method for tuning the domain spacing $(D_{\rm sp})$ of self-assembled block copolymer thin films of poly-(styrene-block-methyl methacrylate) (PS-b-PMMA) over a large range of lamellar periods. By modifying the molecular weight distribution (MWD) shape (including both the breadth and skew) of the PS block via temporal control of polymer chain initiation in anionic polymerization, we observe increases of up to 41% in $D_{\rm sp}$ for polymers with the same overall molecular weight $(M_p \approx 12\hat{5})$ kg mol⁻¹) without significantly changing the overall morphology or chemical composition of the final material. In conjunction with



our experimental efforts, we have utilized concepts from population statistics and least-squares analysis to develop a model for predicting D_{sp} based on the first three moments of the MWDs. This statistical model reproduces experimental D_{sp} values with high fidelity (with mean absolute errors of 1.2 nm or 1.8%) and provides novel physical insight into the individual and collective roles played by the MWD moments in determining this property of interest. This work demonstrates that both MWD breadth and skew have a profound influence over D_{sb} , thereby providing an experimental and conceptual platform for exploiting MWD shape as a simple and modular handle for fine-tuning $D_{\rm sp}$ in block copolymer thin films.

■ INTRODUCTION

The use of block copolymers has become pervasive in the fields of chemistry, materials science, and engineering over the past few decades. With the propensity to rapidly self-assemble into highly ordered nanostructures, block copolymers have played an integral role in the development of novel photonic applications, lithographic materials, filtration membranes, and thermoplastic elastomers. 1-21 However, the ability to control and selectively tune the properties of block copolymers over a broad range without changing their chemical composition remains a challenge to date. For this objective to be addressed, modifying the molecular weight distribution (MWD) of the final material has recently emerged as a promising path forward.²⁶⁻⁵¹ In this regard, a comprehensive understanding of how the MWD shape (e.g., the breadth/ spread, skew, etc.) influences the phase behavior and physical properties of block copolymers is still in its infancy and will be fundamental to the future success of this approach.

Polymers are typically characterized using the following statistical quantities: the number-average molar mass (M_n) , the weight-average molar mass (M_w) , and the dispersity (D), which is defined as the ratio $M_{\rm w}/M_{\rm p}$. The effects of molecular weight on copolymer phase behavior are fairly well understood. 51,52 However, in many instances, such as the fabrication of photonic polymers with very large domain spacing (D_{sp}) , increasing M_n is

not an effective strategy due to the likelihood of chain scissions and other difficulties with the preparation and processing of high molecular weight materials. 54-59 In these cases, it becomes crucial to look at other avenues for tuning phase behavior such as altering the polymer MWDs. To date, only a few research groups have investigated the influence of MWD, or more accurately the D, on the self-assembly of di- and triblock copolymers. 10,35,36,39,40,44,45,60-62 Lynd and Hillmyer found that increasing the D of one block (of a diblock copolymer) results in shifted phase boundaries in block copolymer melts, and Matyjaszewski and co-workers have shown that traditionally metastable morphologies, such as hexagonally perforated layers, can be stabilized with high values of D. Moreover, Mahanthappa and co-workers reported that triblock copolymers with a disperse midblock ($\mathcal{D} \approx 2$) prepared by uncontrolled methods have composition-dependent morphology windows that differ considerably from those of their counterparts with narrow distributions ($\mathcal{D} \approx 1$). Quite interestingly, it has been demonstrated that the incorporation of blocks with large \mathcal{D} influences the D_{sp} of bulk materials. 10,35,39

Received: January 18, 2018 Published: March 9, 2018

[†]Department of Chemistry and Chemical Biology, Cornell University, Ithaca, New York 14853, United States

Department of Materials Science and Engineering, Cornell University, Ithaca, New York 14853, United States

^LCornell High Energy Synchrotron Source (CHESS), Cornell University, Ithaca, New York 14853, United States

However, the manipulation of D is only the first step in harnessing the shape of the MWD in the control and finetuning of block copolymer properties. In this regard, the use of D as the sole statistical quantity to describe a MWD is quite limited as it only defines the relative breadth of molar masses in a polymer sample and therefore provides an incomplete and oversimplified description of the MWD shape. To proceed forward, a more comprehensive characterization of MWD shape will require quantities that incorporate statistical information from higher moments of the distribution such as skewness and kurtosis, which describe the relative degree of asymmetry and population in the tails in a given MWD. Although such quantities have been proposed to heavily influence polymer properties, 22,26-28,34,63-65 experimental validations for such hypotheses have been hindered due to the lack of modular synthetic strategies for gaining predictive control over chain length composition in a MWD. With these synthetic challenges in mind, we have recently reported that temporal regulation of chain initiation in controlled polymerizations does indeed impart deterministic control of the breadth and skew of polymer MWDs (Figure 1), thereby providing an experimental platform for exploiting MWD shape as a simple and modular handle to fine-tune polymer properties.^{26–28}

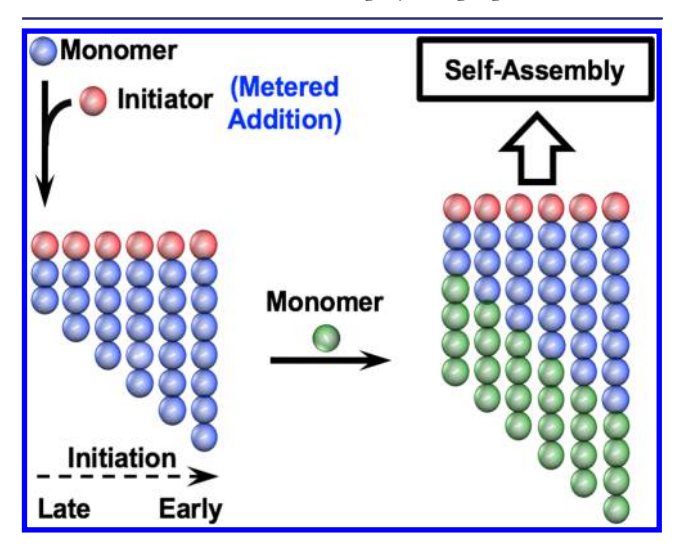


Figure 1. General synthetic strategy for the preparation of block copolymers with controlled MWD breadth and skew via temporal regulation of polymer chain initiation of the first block (blue) followed by chain extension with a second monomer (green) to afford well-defined diblock copolymers.

In this study, we employ the aforementioned synthetic strategy to investigate the self-assembly of poly(styrene-block-methyl methacrylate) (PS-b-PMMA) thin films in which the PS blocks have systematically varied MWD breadths and skews. The general approach is shown in Figure 1. Quite interestingly, we demonstrate that the PS MWD skew has a substantial influence over the phase behavior of PS-b-PMMA with effects that are of the same order of magnitude as the breadth/spread. By only modifying the breadth and skew of the PS block MWD, we observed unprecedented increases in $D_{\rm sp}$ of more than 40% without significantly changing the overall morphology or chemical composition of the final material. To quantify and further differentiate the individual and collective roles played by the MWD breadth and skew in determining $D_{\rm sp}$, we have also developed a highly accurate statistical model for predicting this

quantity based on the first three moments of the MWDs. We anticipate that the findings reported herein on the tailoring of $D_{\rm sp}$ in block copolymers will have significant ramifications in the development of novel photonic polymers, which require atypically large periodicities to scatter light. More broadly speaking, we also hope that this work will provide an experimental and conceptual framework for exploiting MWD shape as a simple and modular handle for fine-tuning the phase behavior and physical properties of block copolymer thin films.

■ RESULTS AND DISCUSSION

Design and Thin Film Self-Assembly. The preparation of PS-*b*-PMMA via anionic polymerization was chosen as a model system due to its living nature, i.e., high chain-end fidelity and the excellent control of molecular weight for both blocks in the polymerization, which allowed the chain-length heterogeneity to be confined to the PS block.^{35,66–69} Figure 2 shows the

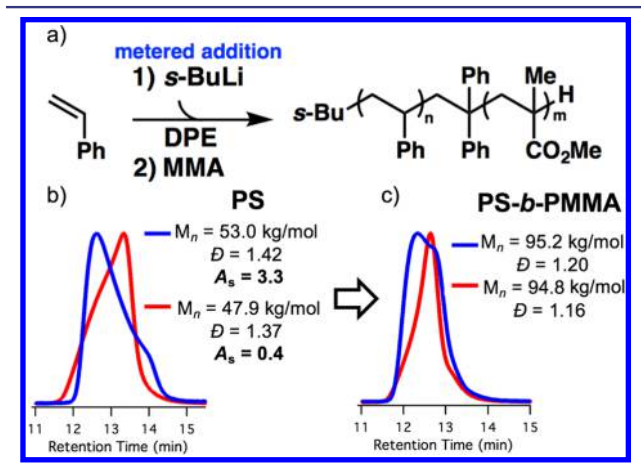


Figure 2. (a) General synthetic approach to PS-b-PMMA diblock copolymers through metered addition of s-BuLi and representative size-exclusion chromatography traces of (b) starting PS blocks and (c) PS-b-PMMA showing the controlled MWD shape of the PS block (DPE, diphenylethylene; PMMA, poly(methyl methacrylate); PS, polystyrene).

general synthetic strategy and representative size-exclusion chromatography (SEC) traces of the diblock copolymers. Slow addition of an alkyllithium initiating species (s-BuLi) to a monomer solution at predetermined rates and times (see Tables S1 and S2) allows for precise temporal control of polymer chain initiation and skews the MWD to either high or low molar mass (Figure 2b). More precisely, a negative skew, or skewing to high molar mass (red PS trace; Figure 2b), represents tailing into the high molecular weight region of the SEC trace while the distribution is tilted toward lower molecular weight (the mode is shifted toward lower molecular weight). Likewise, a positive skew, skewing to low molecular weight (blue PS trace in Figure 2b), describes the shape of a chain length distribution that tails into the low molecular weight region of the SEC trace while the mode is shifted toward higher molecular weight. The M_n of the PS block of all polymers in this study was held constant at \sim 50 kg mol⁻¹, which is controlled via the ratio of monomer to total initiator added to the reaction mixture. Each PS block was subsequently chain-extended with varying amounts of methyl methacrylate until the final block copolymers reached overall M_p values from 75 to 140 kg mol⁻¹ (Figure 2c).

Table 1. Molecular and Morphological Characteristics of PS-b-PMMA Diblock Copolymers

| sample (p) | $M_{ m n,PS} \ ({ m kg~mol}^{-1})$ | $\mathcal{D}_{	ext{PS}}$ | $A_{s,PS}^{a}$ | $M_{ m n,PS-\it b-PMMA} \ m (kg\ mol^{-1})$ | $artheta_{	ext{PS-}b	ext{-PMMA}}$ | $f_{\mathrm{v,PS}}^{b}$ | $\binom{D_{\mathrm{sp,expt}}^c}{(\mathrm{nm})}^c$ | M_1^{d} (min) | M_2^{d} (min) | M_3^{d} (min) | $D_{	ext{sp,pred}}^{}d} onumber (nm)^d$ |
|------------|------------------------------------|--------------------------|----------------|--|-----------------------------------|-------------------------|---|-----------------|-----------------|-----------------|--|
| 1 | 52.6 | 1.10 | N/A | 90.3 | 1.08 | 0.54 | 52.6 | 12.61 | 0.269 | 0.280 | 53.8 |
| 2 | 54.1 | 1.08 | N/A | 91.8 | 1.10 | 0.55 | 53.8 | 12.60 | 0.227 | 0.266 | 54.0 |
| 3 | 52.6 | 1.10 | N/A | 104.7 | 1.10 | 0.46 | 57.9 | 12.48 | 0.269 | 0.280 | 58.4 |
| 4 | 54.1 | 1.08 | N/A | 107.6 | 1.10 | 0.46 | 61.2 | 12.44 | 0.227 | 0.266 | 59.4 |
| 5 | 52.6 | 1.10 | N/A | 113.0 | 1.09 | 0.43 | 62.4 | 12.40 | 0.269 | 0.280 | 62.5 |
| 6 | 54.1 | 1.08 | N/A | 122.0 | 1.11 | 0.40 | 67.6 | 12.31 | 0.227 | 0.266 | 66.5 |
| 7 | 54.1 | 1.08 | N/A | 140.9 | 1.13 | 0.34 | 76.4 | 12.16 | 0.227 | 0.266 | 77.9 |
| 8 | 55.7 | 1.45 | 0.35 | 79.0 | 1.28 | 0.67 | 50.9 | 12.71 | 0.584 | -0.307 | 50.9 |
| 9 | 47.9 | 1.37 | 0.38 | 94.8 | 1.16 | 0.46 | 58.6 | 12.60 | 0.528 | -0.227 | 55.9 |
| 10 | 53.8 | 1.38 | 0.42 | 104.2 | 1.17 | 0.48 | 60.8 | 12.48 | 0.514 | -0.219 | 61.7 |
| 11 | 47.9 | 1.37 | 0.38 | 104.6 | 1.15 | 0.42 | 62.0 | 12.45 | 0.528 | -0.227 | 63.4 |
| 12 | 53.8 | 1.38 | 0.42 | 111.6 | 1.17 | 0.44 | 69.1 | 12.37 | 0.514 | -0.219 | 68.7 |
| 13 | 55.7 | 1.45 | 0.35 | 119.6 | 1.18 | 0.43 | 72.8 | 12.32 | 0.584 | -0.307 | 72.4 |
| 14 | 47.9 | 1.37 | 0.38 | 125.1 | 1.20 | 0.35 | 77.7 | 12.24 | 0.528 | -0.227 | 79.6 |
| 15 | 47.9 | 1.37 | 0.38 | 139.4 | 1.16 | 0.35 | 85.7 | 12.19 | 0.528 | -0.227 | 84.4 |
| 16 | 53.0 | 1.42 | 3.30 | 74.9 | 1.27 | 0.67 | 47.5 | 12.73 | 0.559 | 0.474 | 47.4 |
| 17 | 53.0 | 1.42 | 3.30 | 95.2 | 1.20 | 0.52 | 62.3 | 12.54 | 0.559 | 0.474 | 60.3 |
| 18 | 53.0 | 1.42 | 3.30 | 104.6 | 1.20 | 0.47 | 67.3 | 12.44 | 0.559 | 0.474 | 69.3 |
| 19 | 51.3 | 1.41 | 3.22 | 113.5 | 1.20 | 0.41 | 77.7 | 12.35 | 0.556 | 0.483 | 78.6 |
| 20 | 53.0 | 1.42 | 3.30 | 121.7 | 1.20 | 0.40 | 82.9 | 12.30 | 0.559 | 0.474 | 84.4 |
| 21 | 51.3 | 1.41 | 3.22 | 125.8 | 1.24 | 0.37 | 95.5 | 12.23 | 0.556 | 0.483 | 93.0 |

^aAsymmetry factor (A_s) of the polystyrene (PS) block (vide supra). ^bVolume fraction $(f_{v,PS})$ of the PS block calculated from tabulated homopolymer densities. ^cExperimental and predicted domain spacings $(D_{sp,expt}$ and $D_{sp,pred}$ respectively) of perpendicularly oriented PS-b-PMMA lamellae. ^d M_1 , M_2 , and M_3 denote the descriptors employed in our statistical model that describe the molecular weight distribution shape (first three moments).

Initially, a series of polymers with narrow PS MWDs (Table 1, samples 1–7) and increasing fractions of PMMA was prepared as a control group. Subsequently, a repertoire of polymers with similar overall $M_{\rm n}$ values and block compositions but with PS blocks with broader distributions ($\mathcal{D}\approx 1.4$) and either negative or positive skewing (see Table 1, samples 8–15 and samples 16–21, respectively). We note in passing that the asymmetry factor ($A_{\rm s,PS}$) is included as a qualitative descriptor for the skew of each PS MWD, where $A_{\rm s,PS}$ values of >1 and <1 describe skewing to low and high molar mass, respectively. The fraction of PMMA content was varied across these three sets of polymers to investigate the impact of PS MWD shape on self-assembly at different total molecular weights and block compositions ($f_{\rm v,PS}$ of 0.35–0.65).

Using the library of PS blocks with systematically deviating compositions of chain lengths and increasing fractions of the PMMA blocks between samples, we prepared thin films on silicon wafers and performed grazing-incidence small-angle Xray scattering (GISAXS) studies to determine the morphological characteristics of each block copolymer (Figure 3). As anticipated, polymers with narrow PS MWDs showed modest increases in $D_{\rm sp}$ from 52.6 to 76.4 nm with increasing molar mass from 90.3 to 140.9 kg mol⁻¹ (Figure 3a, green entries). Specifically, an extension in molecular weight of 50.6 kg mol⁻¹ (a 56% increase of overall M_n) resulted in a 23.8 nm increase in $D_{\rm sp}$ (a 45% expansion of the lamellar period). Notably, when $D_{\rm sp}$ was broadened to 1.4 and skewed to high molar mass (Figure 3a, red entries), large increases in $D_{\rm sp}$ were observed relative to those seen for the narrow PS MWD control group. In contrast to block polymers with narrow PS distributions, polymers with negative skew and $M_{\rm n}$ values from 79.0 to 139.4 kg mol⁻¹ showed remarkable increases in $D_{\rm sp}$ from 50.9 to 85.7 nm. This corresponds to a 67% rise over the range of molar masses studied here. Among polymers with similar M_n values (see

Table 1, entries 6 and 14), a \mathcal{D} of 1.4 and MWD skewing of the PS block to high molar mass resulted in increases in block periodicities of up to 15% compared with those of samples with narrow MWDs. These data show that broadening the MWD of one block to a \mathcal{D} of 1.4 has a strong influence on this aspect of phase behavior, resulting in a large increase in the window of available domain periods for polymers with almost identical molar mass and volume fraction.

Most intriguing, when the \mathcal{D} of the PS block was broadened to 1.4 and low molar mass skewing was imparted on the MWD (Figure 3a, blue entries), even larger increases in lamellar periods from 47.5 to 95.5 nm were observed, a 100% expansion in $D_{\rm sp}$ for polymers with $M_{\rm p}$ values between 74.5 and 125.8 kg mol⁻¹. Remarkably, relative to narrow MWD polymers with similar M_n values (see Table 1, entries 6 and 21), polymers with PS blocks skewed to low molar mass showed a 41% enhancement in $D_{\rm sp}$, which is almost 30 nm. This type of skewing allowed access to a $D_{\rm sp}$ of 95.5 nm in a polymer of only 125.8 kg mol⁻¹. Moreover, compared with polymers skewed to high molar mass, those skewed to low molar mass showed a $D_{\rm sp}$ increase of up to 23% at the same \mathcal{D} (samples 14 and 21), demonstrating clearly that PS MWD skew has a profound role in the self-assembly of lamellar domains. We envision that these findings will provide a platform from which to use MWD skew as a useful tool for manipulating the phase behavior of block copolymers.

As an important aside, we note that preparing materials with very large $D_{\rm sp}$ by solely increasing molecular weight has significant fundamental and practical limits. First, the Gaussian chain model for lamellar systems suggests that $D_{\rm sp}$ increases sublinearly with $M_{\rm n}$ in symmetric diblock copolymers. Though this effect is not apparent as plotted in Figure 3 (presumably due to the narrow range of molecular weights and increasing asymmetry in the volume fraction of the polymers in

Journal of the American Chemical Society

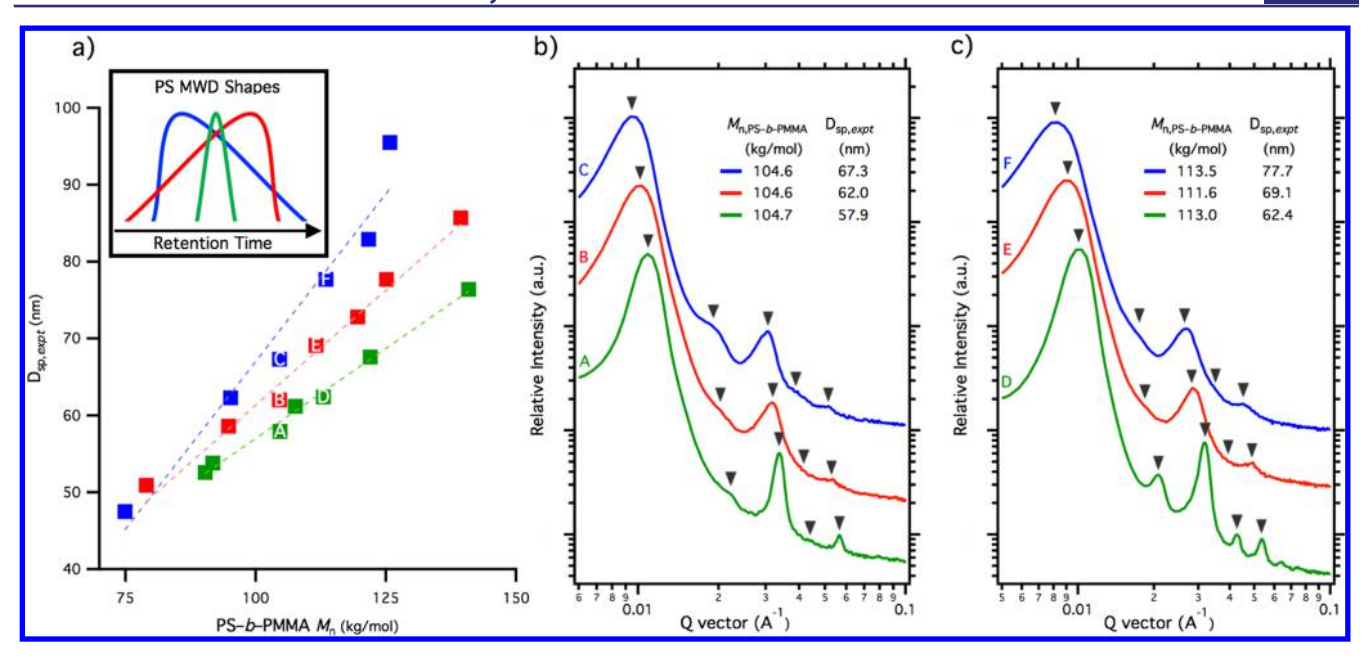


Figure 3. (a) $D_{\rm sp}$ versus overall PS-b-PMMA $M_{\rm n}$ for positively skewed (blue), negatively skewed (red), and narrow MWD (green), which shows vastly different lamellar periods dependent on PS MWD skew. (b, c) Analogous GISAXS line cuts along the Yoneda band plotted versus log Q vector show strong shifts in the primary reflection (first triangle) used to find $D_{\rm sp}$ in (a). Line cuts have been indexed to lamellae.

this study, see Supporting Information), the model brings to light the fact that there exists a plateauing effect on $D_{\rm sp}$. That is to say, as the $M_{\rm n}$ increases, its influence on $D_{\rm sp}$ is reduced. Thus, the molecular weight cannot simply be increased to attain arbitrarily high $D_{\rm sp}$. Moreover, high molecular weight block copolymer chains can have a limited ability to diffuse to form an equilibrium morphological structure and are often trapped in a nonequilibrium state. \$4-57 In addition to the above inherent limits, high molecular weights pose critical processing challenges for two practical reasons. First, high molecular weight materials with narrow MWD often have very high viscosities, requiring a correspondingly high energy input for sufficient melt-processing, and second, these large polymers are prone to chain scissions during such energy-intensive processing, which considerably damages the material and alters its intended physical properties. 58,59,72 Regarding these problems, we envision that our approach will help bridge some of this gap and will, therefore, be the subject of future

Further visualization of this change in $D_{\rm sp}$ with changing PS MWD spread and skew is shown in Figure 3b and c, which present the horizontal GISAXS line cuts of two sets of polymers with similar molar masses but different MWDs of the PS block. Plots of relative intensities versus log of the Q-vector distinctly illustrate large shifts in the primary reflection. The position of these Bragg peaks embodies the extreme influence of the PS MWD shape on $D_{\rm sp}$, which falls to lower Q as PS MWD is broadened and positively skewed. The broadening of the primary and higher-order reflections indicates that some degree of long-range order is lost (or decreasing grain size) as the PS MWD is broadened and/or skewed. However, in most cases, three scattering peaks are observed, demonstrating that the films remain well-ordered. All of the samples we have evaluated here had quantifiable scattering in only the Yoneda band of the two-dimensional scattering pattern (with scattering in the horizontal direction suggesting that the block copolymer interface is primarily oriented normal to the substrate surface). These scattering results reveal only integer value vertical

reflections that are characteristic of perpendicular lamellar morphology (see Figure S7 for representative 2D GISAXS data). $^{53,74-80}$ Notably, this was the only morphology observed

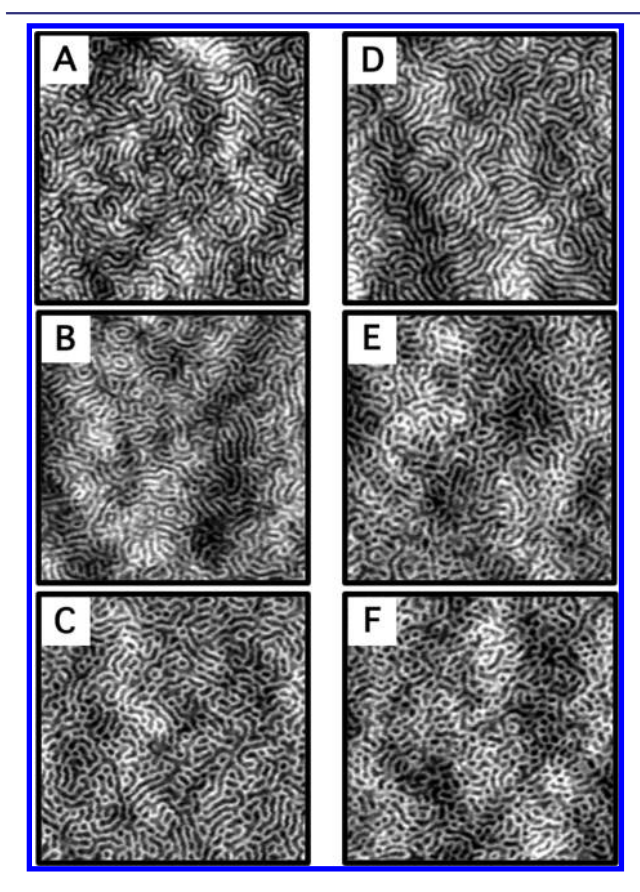


Figure 4. Atomic force microscopy (AFM) height images ($2 \times 2 \mu m$) of unaligned perpendicular lamellae. Sample names (A–F) correspond to those labeled in Figure 2. Fast Fourier Transforms (FFTs) are shown in the Supporting Information.⁷³

in all of the polymers studied here. More interesting, however, is that these modifications to the PS MWD breadth and skew result primarily in large changes to $D_{\rm sp}$ that are not accompanied by a simultaneous phase transition. Apart from reduced grain size, the fact that large variations in MWD shape of the PS block left the overall morphology predominantly intact indicates that this should be a rather durable way to modulate $D_{\rm sp}$ in block copolymer thin films.

Atomic force microscopy studies also lend support to the fact that the overall morphology remains intact (Figure 4) by showing the expected fingerprint pattern for perpendicular meandering lamellae. These micrographs demonstrate that, in addition to the internal morphology, the surface morphology also remains well ordered when the MWD shape of the PS block has been significantly altered.

The origin of domain spacing expansion in samples with large D has been of considerable interest both experimentally and theoretically. The observed increase in lattice spacing of bulk samples with relatively large D has been attributed to the tendency for individual polymer chains to withdraw from the interface and swell the domain of their majority-like segment. 10,30,45,81,82 In general, it is enthalpically most favorable to surround both the A and B blocks by their like segments, which is only possible when each chain is confined to the interface. However, although confining all chains to the 2-dimensional interface minimizes unfavorable A-B contacts, it also imposes a stringent entropic penalty on the polymer chain ensemble. Thus, in a polymer sample with large enough disparities in A-B block lengths (e.g., short A blocks bound to long B blocks, such as found in samples with large D), more stabilization is gained entropically by surrounding small A blocks with dissimilar B segments than is gained enthalpically by confining these chains to the domain interface. Such asymmetric polymer chains, therefore, preferentially diffuse away from the interface and swell the majority B domain, increasing the overall D_{sp} .

We propose that such polymer chain desorption from the interface is a major contributing mechanism to domain swelling in our samples with diverse PS MWD shapes. This hypothesis is initially supported by the fact that broadening the PS MWD to a D of 1.4 results in increased lattice spacing for both positively and negatively skewed samples. Hence, in contrast to narrow MWDs (Table 1, samples 1–7), the presence of low molecular weight PS species in the broad distributions (Table 1, samples 8–21) allows swelling of the PMMA domain to take place. More interesting, the data shown here also clearly demonstrate that this driving force is quite sensitive to the PS MWD shape or the absolute composition of long, medium, and short chains. Because the positively skewed samples have a larger portion of relatively low molecular weight material, the influence of chains withdrawing from the interface is expected to be amplified in these samples relative to those with negatively skewed PS MWDs. Moreover, this hypothesis is also reinforced through the observation that increasing the molecular weight of the PMMA block increases the difference in D_{sp} of positively versus negatively skewed samples. In this case, the growth in molecular weight of the PMMA block would result in the propensity for larger PS chains to be pulled away from the interface, thus permitting a greater number of PS chains to be pulled into the center of the PMMA domain. Because the positively skewed samples have a larger relative portion of low molecular weight species, the disparate rise in $D_{\rm sp}$ for such samples is consistent with the aforementioned hypothesis. Moreover, the observed coalescence of D_{sp} values at lower molecular weights in Figure 3a further supports this proposition and denotes the point at which the PMMA block is too small to drive short PS chains away from the interface. These observations illustrate the sensitivity of domain spacing to the relative population of low molecular weights chains and, consequently, the promising potential of using MWD skew to precisely control such properties.

Lastly, large $\mathcal D$ has also been proposed to influence the overall lamellar spacing by decreasing the entropic cost of stretching an ensemble of chains due to the combination of large and small chains being able to fill space more efficiently. This allows an ensemble of chains to stretch further than its narrow MWD counterpart. More experimental and theoretical evidence is needed to determine the degree to which this mechanism is contributing to the overall $\mathcal D_{\rm sp}$ with respect to the MWD shape of the PS block. 40,45,46,83,84

Statistical Modeling and Least-Squares Analysis. An accurate and reliable quantitative description of how MWD shape influences block copolymer phase behavior would not only provide key physical insight into fundamental quantities such as $D_{\rm sp}$ but also further enable the rational design of block copolymers with new and improved physical properties. As a first step toward achieving this goal, we have employed concepts from population statistics and linear least-squares analysis to construct a model that correlates the statistical descriptors of MWD shape to $D_{\rm sp}$ in block copolymer thin films. S5,86 We envision the use of more sophisticated machine learning-based techniques $^{87-92}$ to further enrich our understanding of the physical consequences of MWD shape in the future when more data becomes available.

To start, we used the unprocessed elution profiles (traces) obtained from size exclusion chromatography (SEC) instead of the differential distributions in an effort to eliminate any potential ambiguities due to postprocessing of the raw SEC data. In our statistical model, we utilized three descriptors (M_1 , M_2 , and M_3) derived from the first three moments of the unprocessed SEC traces to describe the physical MWD variables that have been experimentally modified in this study (i.e., the size of the PS-b-PMMA, the spread of the PS block, and the skew of the PS block).

For the M_1 statistical descriptor, we employed the first moment of the diblock copolymer SEC trace, which represents the overall molecular weight of the PS-b-PMMA. This choice is tantamount to quantifying the increase of PMMA in this diblock copolymer because the M_n of the PS block remained constant throughout this study (with an M_n of 50 kg mol⁻¹; see Table 1). Because the next quantity of interest was the breadth/ spread of the PS block, we took the square root of the second central moment (i.e., the standard deviation) of the PS SEC trace as the M_2 statistical descriptor. For the changes in the skew of the PS block to be captured, the cubic root of the third central moment was used as the M_3 statistical descriptor. The functional form chosen for the M_2 and M_3 descriptors (i.e., the square and cubic roots of the corresponding central moments, respectively) yields a set of statistical quantities with units that are consistent with M_1 . We note in passing that the use of consistent units is one of the requirements for quantifying the relative importance of each of these MWD shape descriptors in determining properties of interest such as $D_{\rm sp}$.

Letting $\rho(t)$ represent the fractional elution rate at time t from a given SEC trace, we know that

$$\int \rho(t) \, \mathrm{d}t = 1 \tag{1}$$

due to normalization. As such, the first raw moment as well as the second and third central moments of a SEC trace are given by

$$\mu_1 = \int \rho(t) \times t \, dt \tag{2}$$

$$\mu_2 = \int \rho(t) \times (t - \mu_1)^2 dt \tag{3}$$

and

$$\mu_3 = \int \rho(t) \times (t - \mu_1)^3 dt \tag{4}$$

respectively. As described above, we seek to construct a set of statistical descriptors that can be used to correlate $D_{\rm sp}$ with the overall molecular weight of the PS-b-PMMA, the breadth/spread of the PS block, and the skew of the PS block. To do so (and still maintain a set with consistent units), the M_1 , M_2 , and M_3 statistical descriptors were taken as

$$M_1 = \mu_1^{\text{PS-}b\text{-PMMA}} \tag{5}$$

$$M_2 = \sqrt[2]{\mu_2^{\text{PS}}} \tag{6}$$

and

$$M_3 = \sqrt[3]{\mu_3^{PS}} \tag{7}$$

respectively (see Table 1). Note that the M_3 statistical descriptor above in eq 7 is not equivalent to the statistical definition of skewness (which is also known as the Pearson's moment coefficient of skewness) given by $\alpha_3 = \mu_3/\mu_2^{3/2}$. In theory, higher central moments could also be used as statistical descriptors. In practice, however, one is often faced with a limited data set and care must be taken to employ the minimal number of descriptors in a statistical model (i.e., to prevent overfitting). With access to an increased number of samples in the future (in this work, we have N=21 polymer samples), it would be very interesting to explore how such higher central moments are correlated with physical properties of interest.

Using these three statistical descriptors, the experimental $D_{\rm sp}$ for a given polymer sample, p, were fit to the following power series expansion

$$D_{\text{sp,expt}}^{(p)} \approx \sum_{ijk} c_{ijk} (\Lambda_1^{(p)})^i (\Lambda_2^{(p)})^j (\Lambda_3^{(p)})^k = D_{\text{sp,pred}}^{(p)}$$
(8)

in which the c_{ijk} are the targeted expansion coefficients, and the sum starts with i=j=k=0 and includes all terms such that $i+j+k\leq \Gamma$, where Γ is the truncation order (which is usually taken to be 1 or 2 in this work). For the p-th polymer sample, $\Lambda_1^{(p)}$, $\Lambda_2^{(p)}$, and $\Lambda_3^{(p)}$ are the normalized deviations for each statistical descriptor from the corresponding population mean, i.e.,

$$\Lambda_q^{(p)} = \frac{M_q^{(p)} - \langle M_q \rangle}{\langle M_q \rangle} \tag{9}$$

for q=1,2,3 and $\langle \cdot \rangle$ denotes an average over all of the samples in the training set. In other words, $\langle M_1 \rangle$ represents the mean retention time across all of the PS-b-PMMA SEC traces, and $\Lambda_1^{(p)}$ represents the normalized deviation of the p-th sample from the population mean. $\langle M_2 \rangle$ represents the mean spread in

the retention time across all of the PS SEC traces, and $\Lambda_2^{(p)}$ represents the normalized deviation of the p-th sample from the population mean spread. $\langle M_3 \rangle$ represents the mean skew in the retention time across all of the PS SEC traces, and $\Lambda_3^{(p)}$ represents the normalized deviation of the p-th sample from the population mean skew.

The simplest statistical model for $D_{\rm sp}$ in the form of eq 8 would have $\Gamma=1$ and would include a constant offset (c_{000}) , which is analogous to the *y*-intercept in linear regression analysis, and a term that is linear in each of the statistical descriptors $(c_{100}, c_{010}, c_{001})$. In this work, we will explore the $\Gamma=2$ statistical model, which also accounts for bilinear coupling between statistical descriptors $(c_{110}, c_{101}, c_{011})$, e.g., coupling between the spread and skew, as well as quadratic contributions from individual descriptors $(c_{200}, c_{020}, c_{002})$.

To determine the optimal expansion coefficients in our statistical model (eq 8), we minimize the sum of squared residuals (errors) between the experimental and predicted $D_{\rm sp}$ values over all training samples, i.e.,

$$\{c_{ijk}\} = \arg\min_{\{c_{ijk}\}} \left\{ \sum_{p=1}^{N} \left(D_{\text{sp,expt}}^{(p)} - D_{\text{sp,pred}}^{(p)} \right)^{2} \right\}$$
(10)

To complete our statistical model for $D_{\rm sp}$ in these block copolymers, each term in eq 8 must be normalized over all of the samples in the training set, which results in a transformation of the $\{c_{ijk}\}$ into their final normalized form $\{\overline{c}_{ijk}\}$. This additional level of normalization allows for a quantitative assessment of the relative importance of each term in our statistical model via direct comparison of the final expansion coefficients. For a detailed derivation of this additional normalization procedure, see the Supporting Information. We stress here that this final normalization is crucial for the physical interpretation of the individual and collective influences that each of these PS MWD shape descriptors have in determining $D_{\rm sp}$ in these block copolymers.

To minimize the number of fitting parameters in our statistical model and prevent overfitting, we only use a limited number of terms in the power series expansion formula in eq 8. In doing so, our statistical model reproduces the experimentally observed $D_{\rm sp}$ values with extremely high fidelity, as shown in the correlation plot in Figure 5 (listed in Table 1). Error analysis including the mean signed error (MSE), mean absolute error (MAE), root-mean-squared error (RMSE), and maximum error (MAXE) are provided in Table 2. With an MSE of 0.0 nm, our statistical model shows no systematic error in the prediction of $D_{\rm sp}$ in this data set. Furthermore, the ability to reproduce experimental $D_{\rm sp}$ values to within 1.2-1.4 nm on average (MAE-RMSE) further demonstrates the accuracy and reliability of this approach. We attribute the error remaining in this model to the limited sample size (N = 21), and it is expected that these residual errors will decrease with a larger and more comprehensive set of polymer MWDs.

The final set of optimized expansion coefficients is provided in Table 3. The first term included in our statistical model is $\overline{c}_{000} = +65.6$, which represents a constant (global offset) $D_{\rm sp}$ value corresponding to a reference polymer sample whose statistical descriptors are given by the population means: $M_1 = \langle M_1 \rangle = 12.426$, $M_2 = \langle M_2 \rangle = 0.446$, and $M_3 = \langle M_3 \rangle = 0.134$. In other words, the reference polymer sample in this statistical model is not an idealized MWD with an exceedingly narrow spread (and no skew) centered around a single $M_{\rm p}$ and instead

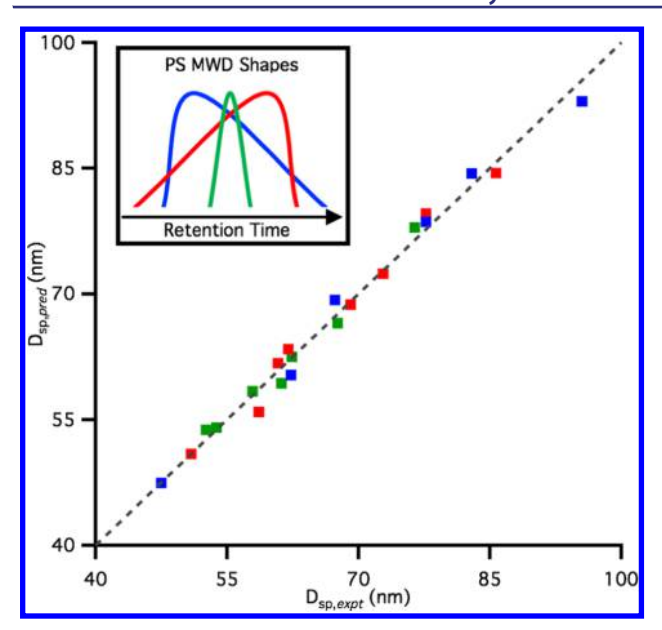


Figure 5. Correlation plot between predicted $(D_{\rm sp,pred})$ and experimental $(D_{\rm sp,expt})$ values based on the statistical model defined in eq. 8. The dashed line represents a perfect correlation.

Table 2. Errors in the Prediction of Domain Spacing (D_{sp})

| | error (nm) |
|------|------------|
| MSE | 0.0 |
| MAE | 1.2 |
| RMSE | 1.4 |
| MAX | 2.7 |
| | |

Table 3. Values and Physical Meanings of the Expansion Coefficients Included in the Statistical Model of Eq 8

| i | j | k | \overline{c}_{ijk} | Physical Meaning |
|---|---|---|----------------------|--|
| 0 | 0 | 0 | +65.6 | constant (global offset) |
| 1 | 0 | 0 | -21.2 | linear (mean, Λ_1) |
| 0 | 1 | 0 | +4.48 | linear (spread, Λ_2) |
| 0 | 0 | 1 | +1.08 | linear (skew, Λ_3) |
| 1 | 1 | 0 | -7.44 | bilinear (mean and spread, $\Lambda_1\Lambda_2$) |
| 1 | 0 | 1 | -5.50 | bilinear (mean and skew, $\Lambda_1\Lambda_3$) |
| 0 | 1 | 1 | +3.02 | bilinear (spread and skew, $\Lambda_2\Lambda_3$) |
| 2 | 0 | 0 | +6.98 | quadratic (mean, $\Lambda_1^2 = \Lambda_1 \Lambda_1$) |

has a slightly broader spread (and small positive skew) that represents the average PS MWD in our sample set.

Consider now the first linear term in our expansion, $\overline{c}_{100} = -21.2$, which represents the correlation between $D_{\rm sp}$ and the mean retention time (of the total diblock copolymer). To physically interpret this finding, note that a negative sign in an expansion coefficient (in the statistical model employed herein) denotes that $D_{\rm sp}$ (i.e., the property of interest) increases with a decrease in the corresponding statistical descriptor. As such, this finding indicates that $D_{\rm sp}$ increases with decreasing retention time. Because of the inverse relationship between retention time and molecular weight, this corresponds to an increase in $D_{\rm sp}$ with increasing molecular weight. This finding aligns well with our current understanding that $D_{\rm sp}$ and polymer molecular weight are positively correlated. The note in passing that a quadratic term in the mean retention time (\overline{c}_{200}) was also included because this statistical descriptor is the most important parameter for determining $D_{\rm sp}$ and

therefore decreases the statistical error in our predictions of this property of interest.

The second linear term in our expansion ($\overline{c}_{010} = +4.48$) accounts for the influence of the spread/breadth in the PS SEC trace and indicates that $D_{\rm sp}$ increases with increasing spread in the retention time. Because this statistical descriptor correlates very well with $D_{\rm PS}$, this finding is again consistent with previous observations that there exists a positive correlation between $D_{\rm sp}$ and $D_{\rm sp}^{-8}$ Interestingly, we note that the magnitude of \overline{c}_{010} (which can be directly compared to the magnitude of \overline{c}_{100} in this statistical model) suggests that, although molecular weight has the largest influence on $D_{\rm sp}$, the influence of PS MWD spread on this property of interest is also quite substantial. In the same breath, we find that the skew of the PS MWD also has a noteworthy influence over $D_{\rm sp}$ as demonstrated by the fact that $\overline{c}_{001} = +1.08$.

In moving beyond $\Gamma=1$, we found that the bilinear couplings in our statistical model (as weighted by the \overline{c}_{110} , \overline{c}_{101} , and \overline{c}_{011} expansion coefficients; see Table 3) are all substantial in magnitude. This finding is strongly indicative of important collective roles played by these MWD descriptors in determining $D_{\rm sp}$. In particular, we note the relatively large bilinear coupling between the mean and skew (with $\overline{c}_{101}=-5.50$) and between spread and skew of the PS block MWD (with $\overline{c}_{011}=3.02$), which suggests that MWD skew has an even more pronounced influence over $D_{\rm sp}$ when the molecular weight and/or MWD spread is also large, as observed experimentally in Figure 3a.

In fact, significant deviations in $D_{\rm sp}$ for polymer samples that have the same overall molecular weight and breadth can be solely attributed to the terms that involve the skew of the PS block MWD. Figure 6 demonstrates this critical finding by plotting the cumulative influence of each term in our statistical model for three samples comprised of similar molecular weights

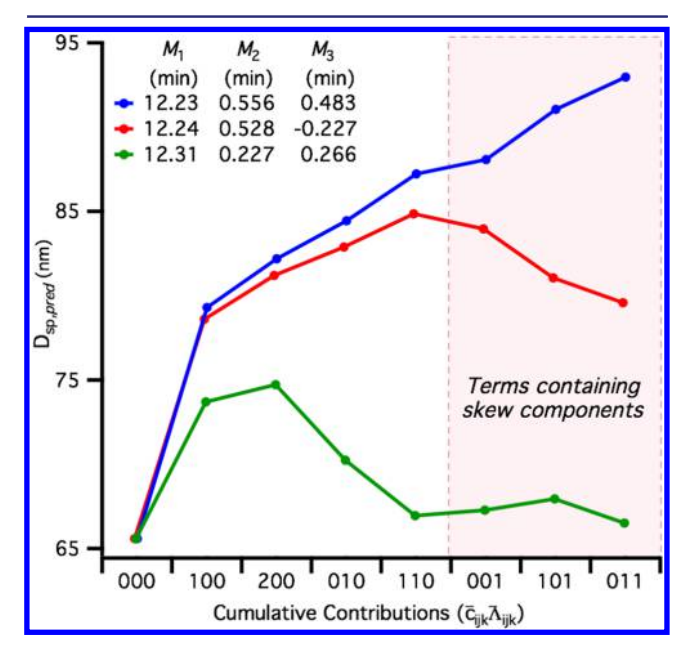


Figure 6. Cumulative contributions to the predicted $D_{\rm sp}$ values for samples 6 (green), 14 (red), and 21 (blue) based on the statistical model defined in eq 8. All samples have the same overall $M_{\rm n}$, and samples 14 and 21 have the same PS MWD breadth and therefore illustrate that large deviations in $D_{\rm sp}$ can be attributed to the skew of the PS block MWD.

and volume fractions. Importantly, our model demonstrates that a narrow PS MWD breadth (Figure 6, green; \overline{c}_{010} and \overline{c}_{110}) results in a decrease in $D_{\rm sp}$ relative to the population average. Further, both positively and negatively skewed PS MWDs have the same distribution breadth (Figure 6, red and blue) and therefore result in similar contributions from the terms containing the distribution mean and spread, as expected. Most interesting, however, are the influences from terms containing a skew component $(\overline{c}_{001}, \overline{c}_{101}, \text{ and } \overline{c}_{011})$. Initially, in the narrow MWD sample with slight positive skew (M_3 = 0.266) close to the population mean ($\langle M_3 \rangle = 0.134$), there is almost no influence of skew in determining the overall $D_{\rm sp}$. Conversely, when the PS MWD is modified and skewed to high (red) or low (blue) molecular weight, the profound influence of MWD shape becomes evident. In this striking example, the predicted D_{sp} values remain essentially the same when only the terms that do not contain a skew component are included. However, once the terms that do account for the PS block skew are included, substantial deviations of ~15 nm emerge in the predicted $D_{\rm sp}$ values. More precisely, a positively skewed PS MWD, which contains a significant portion of low molecular weight polymer chains, leads to an expansion of $D_{\rm sp}$, whereas negatively skewed samples that lack such a fraction of PS chains result in decreased $D_{\rm sp}$ values. These observations are consistent with the hypothesis that domain swelling via chain desorption is sensitive to the relative fraction of low molecular weight chains in the final material, which is governed by MWD skew.

CONCLUSIONS

In this work, we have demonstrated a general approach to using MWD shape (breadth and skew) as a parameter for fine-tuning the $D_{\rm sp}$ of block copolymer thin films. The synthetic process for doing so allows predictable increases in $D_{\rm sp}$ of up to 40% for fairly low molecular weights and relatively narrow dispersity values. GISAXS and AFM studies establish that by tuning the MWD shape of only one block, $D_{\rm sp}$ can be systematically varied across a large window of lamellar periods even at values of the same molecular weight and dispersity. These data illustrate that modulation of the entire MWD may be used as an ever-present handle to fine-tune the phase behavior of the final material. We accompany these experimental results with a robust statistical model that provides a quantitative estimate of the influence of the first three moments of the MWD on domain spacing. This theoretical model illustrates that both breadth and skew have a substantial influence over this property of interest and reproduces the experimental $D_{\rm sp}$ values with high fidelity (to within 1.2–1.4 nm on average). These results show that higher moments of MWDs play an important role in the self-assembly process, and to the best of our knowledge, this work is the first attempt at simultaneously determining the individual and collective influences of MWD mean, spread, and skew on $D_{\rm sp}$ in block copolymers. This joint experimental and theoretical endeavor further expands our fundamental understanding of the critical role played by MWDs in the determination of polymer physical properties. In doing so, we provide an experimental and conceptual platform for exploiting MWD shape as a general and modular handle to fine-tune properties of increasing interest such as $D_{\rm sp}$ in block copolymer thin films. We anticipate that these findings will enable the development of a general and scalable strategy for designing and synthesizing polymers with atypically large periodicities for next-generation photonic materials.

MATERIALS AND METHODS

Preparation of Block Copolymers with Skewed PS Blocks. A 20 mL scintillation vial with a Teflon-coated magnetic stir bar was charged with 8 mL of cyclohexane and 2 mL of styrene (17.5 mmol). Stock solutions of s-BuLi were diluted with cyclohexane to a concentration of 0.1136 M for all reactions. A total volume of 380 μ L was drawn into a 1 mL syringe before mounting on a New Era NE-4000 Double Syringe Pump. The syringe pump was programmed according to the appropriate rate profile (Supporting Information) to dispense 340 μ L of the stock s-BuLi solution into the polymerization. The syringe pump was started immediately after the needle was submerged into the reaction mixture. During initiator addition, the polymerization reaction slowly turned bright orange. After full conversion, diphenylethylene (1.05 equiv) was added and stirred for 1 h until the solution turned deep red.

Chain Extension with MMA and Polymer Isolation. A flamedried Schlenk bomb was brought into the glovebox and charged with LiCl (40 mg, 0.9 mmol). Each Schlenk flask was removed from the glovebox, and 40 mL of tetrahydrofuran was added under positive pressure of argon. Once the LiCl dissolved, the solution was cooled to −78 °C in a dry ice/acetone bath, and a few drops of s-BuLi (1.4 M in cyclohexane) were added until a yellow color persisted. After stirring for 1 h, the solution was warmed to room temperature and maintained until the yellow color dissipated completely. Each Schlenk flask was then brought back into the glovebox, and 2 mL of the living diphenylethyllithium end-capped PS polymerization mixture was added. The flasks were then removed from the glovebox and cooled to -78 °C with dry ice/acetone. Once cooled, the appropriate amount of methyl methacrylate was added under positive pressure of argon, and the flask was sealed and allowed to stir at -78 °C for 1 h before quenching with vigorously degassed methanol. Each polymer was then precipitated into cold methanol, and small amounts of terminated PS homopolymer were removed via Soxhlet extraction with cyclohexane.

Self-Assembly of PS-b-PMMA Thin Films. Silicon wafers were cut to 2 cm × 2 cm, submerged overnight in a piranha solution, rinsed several times with distilled water, and blown dry with nitrogen to remove all visible dust. The wafers were then plasma-treated for 60 s immediately before spin-coating. Each silicon wafer was spun dry from toluene for 30 s at 3000 rpm and an acceleration of 400 s⁻¹. Then, solutions of each polymer in toluene (25 mg/mL) were spun under the same conditions to light blue films, each ~160 nm as measured with a spectroscopic reflectometer (FilMetrics F20). All samples were then thermally annealed in a vacuum oven at 180 °C for 15 h. Although different annealing temperatures were explored, it was determined by AFM that the most well-defined surface morphology was obtained at 180 °C for each type of PS MWD skew used in this study. Longer annealing times did not result in noticeable changes to the surface morphology.

Grazing-Incidence Small-Angle X-ray Scattering. All X-ray experiments were conducted at the D1 beamline of the Cornell High Energy Synchrotron Source (CHESS) with a multilayer monochromator ($\lambda = 1.17$ Å) and a two-dimensional area detector distance of 1.82 m. The critical angle for PS-b-PMMA used in this study was $\alpha_{\rm c,PS-b\text{-}PMMA} \approx 0.11^{\circ}$ and varied slightly from sample to sample. Scattering measurements were obtained at an incident angle of α_i = 0.13°, which is between the critical angle of the polymer film and the ${
m SiO_x/Si}$ substrate ($lpha_{
m c,SiO_x/Si}=0.17^\circ$). Hence, the structure throughout the entire film thickness contributes significantly to the scattering signal via coherent interference. $^{93-95}$ All $D_{\rm sp}$ values were measured at the position of the primary reflection in the GISAXS data from line cuts of the Yoneda band. All GISAXS data was analyzed using Igor's Nika software package.⁹⁸

Statistical Modeling and Least-Squares Analysis. All of the statistical modeling and linear least-squares analyses utilized in this work were performed using an in-house script written in MATLAB 2017b. For computing the moments for each MWD, the SEC traces (which contained intensity vs time data) were mapped via cubic spline interpolation onto an equispaced grid that consisted of 10,000 points and spanned the relevant elution time interval of 9-15 min. All negative intensities from the SEC traces were baseline corrected to zero.

The optimized expansion coefficients in eq 10 were trained on the entire data set (N=21) using least-squares analysis followed by testing on the same data set (with an associated error profile provided in Table 2). To further quantify the error associated with this statistical model, we have also performed leave-one-out (LOO) cross validation within the existing data set. ⁹⁹ In particular, we separated the 21 samples considered herein into 21 distinct training sets (each containing 20 samples) and testing sets (each containing 1 sample). The stability and robustness of our model is confirmed by minimal variation observed in the optimized expansion coefficients during LOO cross validation (with an associated error profile provided in Table S5). To further demonstrate the transferability of our optimized expansion coefficients, we utilized ridge regression (via the introduction of a regularization parameter) during the LOO crossvalidation study and observed no further reduction in the $D_{\rm sp}$ prediction error. 100,101

ASSOCIATED CONTENT

S Supporting Information

The Supporting Information is available free of charge on the ACS Publications website at DOI: 10.1021/jacs.8b00694.

General experimental considerations, detailed procedures, initiator addition profiles, and additional supporting data (PDF)

AUTHOR INFORMATION

Corresponding Authors

*bpf46@cornell.edu

*distasio@cornell.edu

ORCID

Katherine P. Barteau: 0000-0002-8479-5407 Detlef-M. Smilgies: 0000-0001-9351-581X Brett P. Fors: 0000-0002-2222-3825

Author Contributions

[‡]D.T.G. and J.J. contributed equally to this work.

Notes

The authors declare no competing financial interest.

ACKNOWLEDGMENTS

This study was supported in part by the Cornell Center for Materials Research (CCMR) through the NSF MRSEC program (DMR-1719875) and through the Research Experience for Undergraduates program (DMR-1460428). This work was also supported by 3M through a nontenured faculty award. The authors also acknowledge Cornell High Energy Synchrotron Source (CHESS), which is supported by the NSF and National Institutes of Health/National Institute of General Medical Sciences under NSF award DMR-1332208. This research used resources of the National Energy Research Scientific Computing Center, which is supported by the Office of Science of the U.S. Department of Energy under Contract No. DE-AC02-05CH112. Lastly, this work made use of the Cornell NMR Facility, which is supported, in part, by the NSF through MRI award CHE-1531632.

REFERENCES

- (1) Bates, F. S.; Hillmyer, M. A.; Lodge, T. P.; Bates, C. M.; Delaney, K. T.; Fredrickson, G. H. *Science* **2012**, *336*, 434.
- (2) Kim, H.-C.; Park, S.-M.; Hinsberg, W. D. Chem. Rev. 2010, 110, 146.

- (3) Bates, F. S.; Fredrickson, G. H. Annu. Rev. Phys. Chem. 1990, 41, 525.
- (4) Leibler, L. Macromolecules 1980, 13, 1602.
- (5) Fink, Y.; Urbas, A. M.; Bawendi, M. G.; Joannopoulos, J. D.; Thomas, E. L. J. Lightwave Technol. 1999, 17, 1963.
- (6) Stefik, M.; Guldin, S.; Vignolini, S.; Wiesner, U.; Steiner, U. Chem. Soc. Rev. 2015, 44, 5076.
- (7) Kang, Y.; Walish, J. J.; Gorishnyy, T.; Thomas, E. L. Nat. Mater. 2007, 6, 957.
- (8) Kang, C.; Kim, E.; Baek, H.; Hwang, K.; Kwak, D.; Kang, Y.; Thomas, E. L. J. Am. Chem. Soc. 2009, 131, 7538.
- (9) Urbas, A. M.; Maldovan, M.; DeRege, P.; Thomas, E. L. Adv. Mater. 2002, 14, 1850.
- (10) Hustad, P. D.; Marchand, G. R.; Garcia-Meitin, E. I.; Roberts, P. L.; Weinhold, J. D. *Macromolecules* **2009**, *42*, 3788.
- (11) Park, M. Science 1997, 276, 1401.
- (12) Bang, J.; Jeong, U.; Yeol Ryu, Du; Russell, T. P.; Erren, T. C.; Hawker, C. J. Adv. Mater. 2009, 21, 4769.
- (13) Ruiz, R.; Kang, H.; Detcheverry, F. A.; Dobisz, E.; Kercher, D. S.; Albrecht, T. R.; de Pablo, J. J.; Nealey, P. F. Science 2008, 321, 936.
- (14) Kim, S. O.; Harun, H. S.; Stoykovich, M. P.; Ferrier, N. J.; de Pablo, J. J.; Nealey, P. F. *Nature* **2003**, 424, 411.
- (15) Chen, L.; Phillip, W. A.; Cussler, E. L.; Hillmyer, M. A. J. Am. Chem. Soc. 2007, 129, 13786.
- (16) Jackson, E. A.; Hillmyer, M. A. ACS Nano 2010, 4, 3548.
- (17) Ahn, H.; Park, S.; Kim, S.-W.; Yoo, P. J.; Ryu, D. Y.; Russell, T. P. ACS Nano 2014, 8, 11745.
- (18) Zhao, D.; Feng, J.; Huo, Q.; Melosh, N.; Fredrickson, G. H.; Chmelka, F.; Stucky, G. D. Science 1998, 279, 548.
- (19) Liang, C.; Hong, K.; Guiochon, G. A.; Mays, J. W.; Dai, S. Angew. Chem., Int. Ed. 2004, 43, 5785.
- (20) Honeker, C. C.; Thomas, E. L. Chem. Mater. 1996, 8, 1702.
- (21) Quirk, R. P.; Morton, M. In *Thermoplastic Elastomers*, 2nd ed.; Hanser Publishers: New York, 1996; pp 72–100.
- (22) Lynd, N. A.; Meuler, A. J.; Hillmyer, M. A. Prog. Polym. Sci. 2008, 33, 875.
- (23) Grubbs, R. B.; Grubbs, R. H. Macromolecules 2017, 50, 6979.
- (24) Rubber Industry Sees Value in MWD. Chem. Eng. News. 1965, 43, 40.
- (25) Peplow, M. Nature 2016, 536, 266.
- (26) Gentekos, D. T.; Dupuis, L. N.; Fors, B. P. J. Am. Chem. Soc. **2016**, 138, 1848.
- (27) Kottisch, V.; Gentekos, D. T.; Fors, B. P. ACS Macro Lett. 2016, 5, 796.
- (28) Nadgorny, M.; Gentekos, D. T.; Xiao, Z.; Singleton, S. P.; Fors, B. P.; Connal, L. A. Macromol. Rapid Commun. 2017, 38, 1700352.
- (29) Sides, S. W.; Fredrickson, G. H. J. Chem. Phys. 2004, 121, 4974.
- (30) Widin, J. M.; Schmitt, A. K.; Schmitt, A. L.; Im, K.; Mahanthappa, M. K. J. Am. Chem. Soc. 2012, 134, 3834.
- (31) Matsen, M. W. Phys. Rev. Lett. 2007, 99, 148304.
- (32) Leibler, L.; Benoit, H. Polymer 1981, 22, 195.
- (33) Burger, C.; Ruland, W.; Semenov, A. N. *Macromolecules* **1990**, 23, 3339.
- (34) Meuler, A. J.; Ellison, C. J.; Evans, C. M.; Hillmyer, M. A.; Bates, F. S. *Macromolecules* **2007**, *40*, 7072.
- (35) Lynd, N. A.; Hillmyer, M. A. Macromolecules 2007, 40, 8050.
- (36) Widin, J. M.; Kim, M.; Schmitt, A. K.; Han, E.; Gopalan, P.; Mahanthappa, M. K. *Macromolecules* **2013**, *46*, 4472.
- (37) Bendejacq, D.; Ponsinet, V.; Joanicot, M.; Loo, Y. L.; Register, R. A. *Macromolecules* **2002**, *35*, 6645.
- (38) Kennemur, J. G.; Yao, L.; Bates, F. S.; Hillmyer, M. A. *Macromolecules* **2014**, 47, 1411.
- (39) Schmitt, A. K.; Mahanthappa, M. K. Macromolecules 2014, 47, 4346.
- (40) Lynd, N. A.; Hillmyer, M. A. Macromolecules 2005, 38, 8803.
- (41) Vanderlaan, M. E.; Hillmyer, M. A. Macromolecules 2016, 49, 8031.
- (42) Li, S.; Register, R. A.; Weinhold, J. D.; Landes, B. G. Macromolecules 2012, 45, 5773.

- (43) Schmitt, A. L.; Repollet-Pedrosa, M. H.; Mahanthappa, M. K. ACS Macro Lett. 2012, 1, 300.
- (44) Ruzette, A.; Tence-Girault, S.; Leibler, L.; Chauvin, F.; Bertin, D.; Guerret, O.; Gerard, P. *Macromolecules* **2006**, *39*, 5804.
- (45) Matsen, M. W. Eur. Phys. J. E: Soft Matter Biol. Phys. 2006, 21, 199.
- (46) Cooke, D. M.; Shi, A. Macromolecules 2006, 39, 6661.
- (47) Jiang, Y.; Yan, X.; Liang, H.; Shi, A.-C. J. Phys. Chem. B 2005, 109, 21047.
- (48) Jiang, Y.; Huang, R.; Liang, H. J. Chem. Phys. 2005, 123, 124906.
- (49) Pandav, G.; Ganesan, V. J. Chem. Phys. 2013, 139, 214905.
- (50) Doncom, K. E. B.; Blackman, L. D.; Wright, D. B.; Gibson, M. I.; O'Reilly, R. K. Chem. Soc. Rev. **2017**, *46*, 4119.
- (51) Oschmann, B.; Lawrence, J.; Schulze, M. W.; Ren, J. M.; Anastasaki, A.; Luo, Y.; Nothling, M. D.; Pester, C. W.; Delaney, D. R.; Connal, L. A.; McGrath, A. J.; Clark, P. G.; Bates, C. M.; Hawker, C. J. ACS Macro Lett. 2017, 6, 668.
- (52) Matsushita, Y.; Mori, K.; Saguchi, R.; Nakao, Y.; Noda, I.; Nagasawa, M. *Macromolecules* **1990**, 23, 4313.
- (53) Busch, P.; Posselt, D.; Smilgies, D. M.; Rheinländer, B.; Kremer, F.; Papadakis, C. M. *Macromolecules* **2003**, *36*, 8717.
- (54) Runge, M. B.; Bowden, N. B. J. Am. Chem. Soc. 2007, 129, 10551.
- (55) Yoon, J.; Lee, W.; Thomas, E. L. Adv. Mater. 2006, 18, 2691.
- (56) Kim, E.; Ahn, H.; Park, S.; Lee, H.; Lee, M.; Lee, S.; Kim, T.; Kwak, E.; Lee, J. H.; Lei, X.; Huh, J.; Bang, J.; Lee, B.; Ryu, D. Y. ACS Nano 2013, 7, 1952.
- (57) Grubbs, R. B.; Grubbs, R. H. Macromolecules 2017, 50, 6979.
- (58) Nichetti, D.; Manas-Zloczower, I. Polym. Eng. Sci. 1999, 39, 887.
- (59) Perego, G.; Cella, G. D.; Bastioli, C. J. Appl. Polym. Sci. 1996, 59, 37.
- (60) Broseta, D.; Fredrickson, G. H.; Helfand, E.; Leibler, L. Macromolecules 1990, 23, 132.
- (61) Anastasiadis, S. H.; Gancarz, I.; Koberstein, F. T. Macromolecules 1988, 21, 2980.
- (62) Peters, A. J.; Lawson, R. A.; Ludovice, P. J.; Henderson, C. L. *Proc. SPIE* **2013**, 868020.
- (63) Listak, J.; Jakubowski, W.; Mueller, L.; Plichta, A.; Matyjaszewski, K.; Bockstaller, M. R. Macromolecules 2008, 41, 5919.
- (64) Widin, J. M.; Kim, M.; Schmitt, A. K.; Han, E.; Gopalan, P.; Mahanthappa, M. K. *Macromolecules* **2013**, *46*, 4472.
- (65) Lynd, N. A.; Hillmyer, M. A.; Matsen, M. W. Macromolecules 2008, 41, 4531.
- (66) Baskaran, D.; Müller, A. H. E. Prog. Polym. Sci. 2007, 32, 173.
- (67) Young, R. N.; Quirk, R. P.; Fetters, L. J. In Anionic Polymerization; Springer: Berlin; Heidelberg, 1984.
- (68) Hadjichristidis, N.; Pitsikalis, M.; Pispas, S.; Iatrou, H. Chem. Rev. 2001, 101, 3747.
- (69) Hadjichristidis, N.; Iatrou, H.; Pitsikalis, M.; Pispas, S.; Avgeropoulos, A. *Prog. Polym. Sci.* **2005**, *30*, *725*.
- (70) Kirkland, J. J.; Yau, W. W.; Stoklosa, H. J.; Dilks, C. H., Jr J. Chromatogr. Sci. 1977, 15, 303.
- (71) Rudin, A. J. Chem. Educ. 1969, 46, 595.
- (72) Gonzalez-Gonzalez, V. A.; Neira-Velazquez, G.; Angulo-Sanchez, J. L. *Polym. Degrad. Stab.* **1998**, *60*, 33.
- (73) Zhang, X.; Berry, B. C.; Yager, K. G.; Kim, S.; Jones, R. L.; Satija, S.; Pickel, D. L.; Douglas, J. F.; Karim, A. ACS Nano **2008**, *2*, 2331.
- (74) Zhang, J.; Posselt, D.; Smilgies, D. M.; Perlich, J.; Kyriakos, K.; Jaksch, S.; Papadakis, C. M. *Macromolecules* **2014**, *47*, 5711.
- (75) Sepe, A.; Hoppe, E. T.; Jaksch, S.; Magerl, D.; Zhong, Q.; Perlich, J.; Posselt, D.; Smilgies, D.-M.; Papadakis, C. M. J. Phys.: Condens. Matter 2011, 23, 254213.
- (76) Walton, D. G.; Kellogg, G. J.; Mayes, A. M.; Lambooy, P.; Russell, T. P. Macromolecules 1994, 27, 6225.
- (77) Zhang, X.; Douglas, J. F.; Jones, R. L. Soft Matter 2012, 8, 4980.
- (78) Busch, P.; Posselt, D.; Smilgies, D.-M.; Rauscher, M.; Papadakis, C. M. *Macromolecules* **2007**, *40*, 630.
- (79) Potemkin, I. I.; Busch, P.; Smilgies, D.-M.; Posselt, D.; Papadakis, C. M. Macromol. Rapid Commun. 2007, 28, 579.

- (80) Matsen, M. W.; Bates, F. S. Macromolecules 1996, 29, 1091.
- (81) Broseta, D.; Fredrickson, G. H.; Helfand, E.; Leibler, L. *Macromolecules* **1990**, 23, 132.
- (82) Fredrickson, G. H.; Sides, S. W. Macromolecules 2003, 36, 5415.
- (83) Woo, S.; Shin, T. J.; Choe, Y.; Lee, H.; Huh, J.; Bang, J. Soft Matter 2017, 13, 5527.
- (84) Milner, S. T.; Witten, T. A.; Cates, M. E. Macromolecules 1989, 22, 853.
- (85) Devore, J. L. In Probability and Statistics for Engineering and the Sciences; Cengage Learning: Boston, MA, 2015.
- (86) Taylor, J. R. In Introduction to Error Analysis: The Study of Uncertainties in Physical Measurements; University Science Books: South Orange, NJ, 1997.
- (87) Rupp, M.; Tkatchenko, A.; Müller, K.-R.; von Lilienfeld, O. A. Phys. Rev. Lett. **2012**, 108, 058301.
- (88) Bartók, A. P.; Payne, M. C.; Kondor, R.; Csányi, G. Phys. Rev. Lett. 2010, 104, 136403.
- (89) Rajan, K. Mater. Today; Elsevier Ltd: Amsterdam, Netherlands, 2005; Vol. 8, p 38.
- (90) Behler, J.; Parrinello, M. Phys. Rev. Lett. 2007, 98, 146401.
- (91) Hamdia, K. M.; Lahmer, T.; Nguyen-Thoi, T.; Rabczuk, T. Comput. Mater. Sci. 2015, 102, 304.
- (92) Pilania, G.; Wang, C.; Jiang, X.; Rajasekaran, S.; Ramprasad, R. Sci. Rep. 2013, 3, 2810.
- (93) Smilgies, D. M.; Busch, P.; Papadakis, C. M.; Posselt, D. Synchrotron Radiat. News 2002, 15, 35.
- (94) Chavis, M. A.; Smilgies, D.-M.; Wiesner, U. B.; Ober, C. K. Adv. Funct. Mater. 2015. 25. 3057.
- (95) Kim, S. H.; Misner, M. J.; Xu, T.; Kimura, M.; Russell, T. P. Adv. Mater. **2004**, 16, 226.
- (96) Lee, B.; Park, I.; Yoon, J.; Park, S.; Kim, J.; Kim, K.-W.; Chang, T.; Ree, M. *Macromolecules* **2005**, 38, 4311.
- (97) Busch, P.; Rauscher, M.; Smilgies, D. M.; Posselt, D.; Papadakis, C. M. J. Appl. Crystallogr. 2006, 39, 433.
- (98) Ilavsky, J. J. Appl. Crystallogr. **2012**, 45, 324.
- (99) Arlot, S.; Celisse, A. Statist. Surv. 2010, 4, 40.
- (100) Hoerl, A. E.; Kennard, R. Technometrics 1970, 12, 55.
- (101) Seber, G.; Lee, A. J. In Linear Regression Analysis; NJ, 2003.